A VISUAL SERVOING APPROACH TO CONTROL AGRICULTURAL MOBILE MACHINES.

C. DEBAIN*, D. KHADRAOUI**, M. BERDUCAT*, P. MARTINET**, P. BONTON**.

*CEMAGREF
FRENCH INSTITUTE OF AGRICULTURAL AND ENVIRONMENTAL ENGINEERING RESEARCH
CLERMONT-FERRAND REGIONAL CENTRE
03150 Montoldre, France
Tel. : 70 45 03 12
Fax.: 70 45 19 46
email : montoldrc@lyon.cemagref.fr

**LASMEA
Blaise Pascal University of Clermont-Ferrand
U.R.A. 1793 of the C.N.R.S.
Les Cézeaux, 24 Avenue des Landais
63177 Aubière cedex, France
Tel. : 73 40 72 50
Fax. : 73 40 72 62
email : khadra@lasmea.univ-bpclermont.fr

Abstract : **We present experimental results of a visual servoing approach to control an agricultural mobile machine. To detect the limit between mowed and unmowed natural zones, we use an original region segmentation algorithm based on a Markovian modeling of a set of sites. With the 2D informations extracted by the image processing algorithm, a visual servoing unit allows the machine to follow the detected limit. All these algorithms are implanted on a parallel architecture [2].**

INTRODUCTION.

In the domain of mobile robots, the perception of the environment which is necessary for moving robots is often realized by an artificial vision system [7]. In the case of a monocular vision, informations extracted from the image are given by the camera frame. Currently, most of control algorithms combined with artificial vision are calculated in the space linked to the scene. This means a 3D estimation using the 2D visual information extracted from the image processing system. However new techniques of control such as visual servoing are able to control a robot directly in the space linked to the visual perception sensor [4].

The study presented in this paper has been realized for a vehicle which has its director wheels placed at the rear. This machine is used to cut vegetation for instance. The objective of our work, is to detect the limit between mowed and unmowed zones represented as a straight line, then to control the machine with respect to this limit (figure n°1).

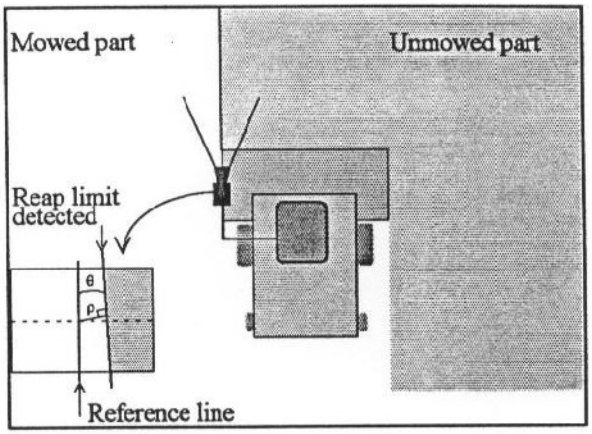

Figure n°1 : a view of our application.

I/ NATURE OF INFORMATION USED BY THE CONTROL. [1][2]

The guidance system uses only the result of reap limit detection between mowed/unmowed natural zones. Represented in the form of a straight line, this visual primitive will constitute the basis information of the control system. An essential phase of the project has therefore been the development of an interface extraction algorithm sufficiently robust to adapt itself to very varied work conditions met in natural environment (nature and height of vegetation, conditions of sunshine...). This objective has been reached by the development of a non supervised algorithm of segmentation in homogeneous regions. This segmentation, based on a Markovian process, uses texture and grey levels data calculated on 16x16 pixels size elementary regions by the means of co-occurrence matrices.

One of the interests of this segmentation in an image sequence, is inherent to the use of the result issued from the previous image. An a priori information is taken into account in the image segmentation. This constitutes the "dynamic" aspect, which consists in putting in relation the extracted data of the new image with the label field of the previous image. Obviously, it has been considered that there are only little changes between two images, in the motion meaning, and a noticeable gain of time is obtained for an equivalent segmentation efficiency.

On the picture n°1, we present an example of segmentation of an image :

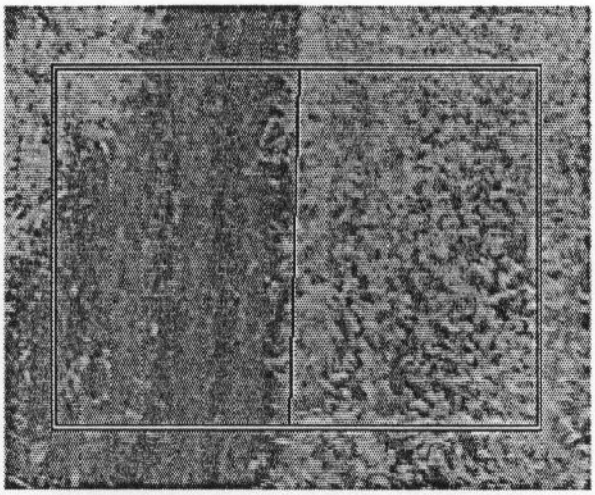

Picture n°1 : a result of image processing.

On this image we can see that the image processing algorithm find the limit between mowed and unmowed vegetation which is represented by a straight line whose polar coordinates are (θ, ρ).

II/ CONTROL LAW.

II.1/ Modelling of the scene [3], [7] :

The aim of this part is to find a relation between the scene and the image .
In this modelling, we use a camera whose focal lenght is equal to unity.

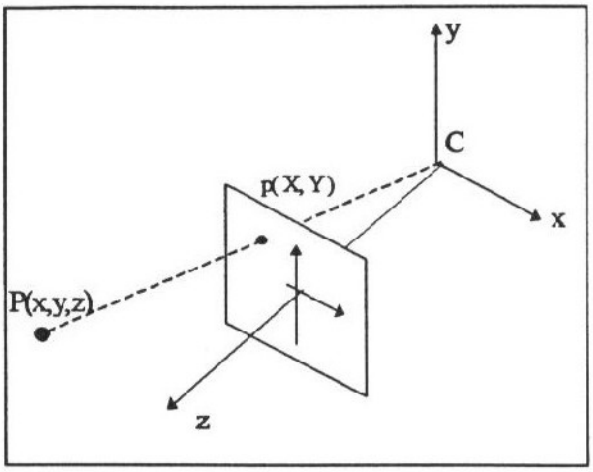

Figure n°2 : perspective projection

On the figure n°2, we show the projection of the 3D scene on the image frame.
The point P(x, y, z) projects onto the image plane as a point p with coordinates (X,Y) (figure n°2) such as :

$$\begin{cases} X = x/z \\ Y = y/z \end{cases} \qquad (1)$$

Knowing the camera velocity vector T, defined by three translational velocities and three rotational ones $T=(V_X, V_y, V_Z, \Omega_X, \Omega_y, \Omega_Z)$, this corresponds to the motion of the object in the 3D scene. These velocities can be expressed by the velocity screw T by means of :

$$\dot{\underline{P}} = -\underline{V} - \underline{\Omega} \wedge \underline{P} \qquad (2)$$

By differentiating (1) and using (2), we can derive the welknown equation relating, optical flow measurement to 3D structure and motion in the scene. We have :

$$\begin{pmatrix} \dot{X} \\ \dot{Y} \end{pmatrix} = L_{of}^{T} \cdot T \qquad (4) \qquad \text{with :}$$

$$L_{of}^{T} = \begin{pmatrix} -1/z & 0 & X/z & X \cdot Y & -(1+X^2) & Y \\ 0 & -1/z & Y/z & (1+Y^2) & -X \cdot Y & -X \end{pmatrix}$$

This equation gives us an interaction relation between the 2D world (image frame) and the 3D one (Object frame).

General method of computing interaction matrix :

In general, a 3D geometrical primitive can be represented as a vectorial function :

$$h(x,y,z,Q_i)=0$$

this one is projected in the image frame under the form :

$$g(X,Y,R_i)=0$$

Where Q_i and R_i are the parameters of the primitives respectively in the 3D scene and in the 2D image plane. From these assumptions, we can establish the interaction screw H_i between primitive R_i and the velocity screw $T=(V_x, V_y, V_z, \Omega_x, \Omega_y, \Omega_z)$. The set of elements H_i is grouped under the matrix L_s assuming that s represents the set of 2D primitives R_i . This matrix is computed assuming the following hypothesis :

$$\begin{cases} g(X,Y,R_i)=0 \\ \dot{g}(X,Y,R_i)=0 \end{cases} \quad (5)$$

After developments, we obtain :

$$\sum_{i=1}^{n} \frac{\partial g}{\partial R_i}\cdot \dot{R}_i = -\frac{\partial g}{\partial X}\cdot \dot{X} - \frac{\partial g}{\partial Y}\cdot \dot{Y} \quad (6)$$

Equation (6) allows us to relate the variation of the parameters $\dot{R}_i$ to the optic flow components L_{of}^{T} and thus, to the velocity screw T of the camera by means of equation (4).

Case of lines :

In 3D frame, a line is defined by two plans which intersect :

$$\begin{cases} a_1x+b_1y+c_1z+d_1=0 \\ a_2x+b_2y+c_2z+d_2=0 \end{cases} \quad (7)$$

By using perspective projection, we obtain :

$$\frac{a_ix+b_iy+c_iz}{d_i} = -\frac{1}{z} \quad (8)$$

In the 2D frame, the equation of the line is :

$$AX+BY+C=0 \quad \text{with :}$$
$$\begin{cases} A=(a_1d_2-a_2d_1) \\ B=(b_1d_2-b_2d_1) \\ C=(c_1d_2-c_2d_1) \end{cases} \quad (9)$$

In the case of (ρ, θ) parametrisation of the line we have :

$$g(X,Y,R)=\rho - X\cos\theta - Y\sin\theta = 0 \quad (10)$$

$$\text{with :} \begin{cases} \theta = \arctan\dfrac{B}{A} \\ \rho = \dfrac{-C}{\sqrt{A^2+B^2}} \end{cases}$$

With (6) and (10) we find :

$$\dot{\rho} + (X\sin\theta - Y\cos\theta)\cdot\dot{\theta} = \dot{X}\cdot\cos\theta + Y\cdot\sin\theta$$

With substituting the expression of X and 1/z, according to Y, in the equation of optical flow, we find by identifying term to term, expression of interaction matrix.

So, we can write :

$$\begin{pmatrix} \dot{\theta} \\ \dot{\rho} \end{pmatrix} = L_{of}^{T}\cdot T$$

with :

$$L_{of} = \begin{pmatrix} \lambda_\theta\cdot\cos\theta & \lambda_\theta\cdot\sin\theta & -\lambda_\theta\cdot\rho \\ \lambda_\rho\cdot\cos\theta & \lambda_\rho\cdot\sin\theta & -\lambda_\rho\cdot\rho \\ -\rho\cdot\cos\theta & -\rho\cdot\sin\theta & -1 \\ (1+\rho^2)\cdot\sin\theta & -(1+\rho^2)\cdot\cos\theta & 0 \end{pmatrix}$$

(11)

and :

$$\begin{cases} \lambda_\theta = (-b_i\cdot\cos\theta + a_i\cdot\sin\theta)/d_i \\ \lambda_\rho = (a_i\cdot\rho\cdot\cos\theta + b_i\cdot\rho\cdot\sin\theta + c_i)/d_i \end{cases}$$

This represents a relation between a line in real scene and a line in the image. The idea is to control our machine with the difference between the line detected and the reference line to reach in the image.

Interaction screw for our application.

The aim of our application is to control our machine on a limit between mowed and unmowed zones of vegetation.

Contrary to the works which has been done on the white line [3], we have only one reference line. So we have to calculate the interaction screw for this line.

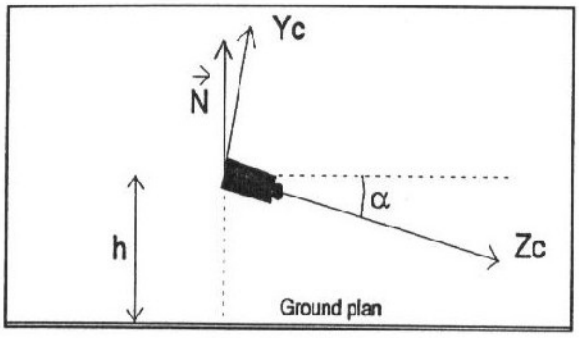

Figure n°3 :Camera and reference line position.

Equation of the plan of the ground in the camera frame :

$\vec{N}$ is a perpendicular vector of the plan of the ground :

$$\vec{N}\begin{pmatrix}0\\ \cos\alpha\\ -\sin\alpha\end{pmatrix}$$

So the plan equation is expressed by:

$$(\cos\alpha).y-(\sin\alpha).z+cte=0$$

M is a point of the plan : $M\begin{pmatrix}0\\ -h/\cos\alpha\\ 0\end{pmatrix}$

Finally we find :

$$(\cos\alpha).y-(\sin\alpha).z+h=0 \qquad (12)$$

Equation of the reference line in polar coordinates :

In the camera frame the equation of the reference line is :

$$\begin{cases}(\cos\alpha).y-(\sin\alpha).z+h=0\\ x=0\end{cases} \qquad (13)$$

So the equation of this line in the image frame and in polar coordinates is:

$$\begin{cases}\rho=0\\ \theta=0\end{cases} (14)$$

$\rho^*=\rho=0$ and $\theta^*=\theta=0$ are the coordinates of the reference line in the polar image frame.

With (14) and (11) we find :

$$\Longrightarrow \lambda_\theta=\frac{1}{h}(-(\cos\alpha))$$

$$\lambda_\rho=\frac{1}{h}(-(\sin\alpha)) \qquad (15)$$

With (11) and (15) we determine the interaction screw for our application. Lots of elements are equal to 0 so there are not in the matrix. :

$$L^T=\begin{pmatrix}-\frac{(\cos\alpha)}{h} & 0 & -1\\ -\frac{(\sin\alpha)}{h} & -1 & 0\end{pmatrix} \qquad \text{with : } T_c\begin{pmatrix}V_x\\ \Omega_y\\ \Omega_z\end{pmatrix}$$

(16)

With this interaction screw we determine a control law [9] :

$$\boxed{T_{control}=-\lambda\cdot L_{of}^{T+}\cdot\left(S-S^*\right)} \qquad (17)$$

$S\begin{pmatrix}\theta\\ \rho\end{pmatrix}$ is the detected line coordinates and $S^*\begin{pmatrix}\theta^*\\ \rho^*\end{pmatrix}$ the coordinates of the reference line.

With the development of the equation (17) we obtain a control of the rotation of our machine in the ground plan :

$$\boxed{\Omega_y=\lambda\cdot\left(-\tan\alpha\cdot\left(\theta-\theta^*\right)+\left(\rho-\rho^*\right)\right)}$$

(18)

This rotation gives the orientation of our vehicle. In fact we just want to control this orientation so we didn't expressed the other equations.

We have a non-holonomic machine, so the difficulty is to make a link between the vehicle orientation and its controls.

II 2/ Kinematic equation of the robot.

We use, a machine which has two wheels steering and two wheels drive (like a car). At constant steering angle, this machine runs on a circle. So, our idea is to replace the machine by an axle which runs on the same circle (figure n°4).

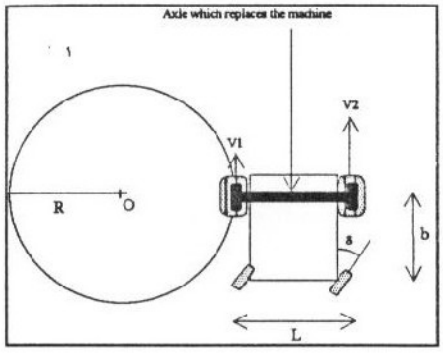

Figure n°4 : Vehicle trajectory.

There is a relation between the angle of this axle and the speed of these wheels [5].
We have (figure n°5) :

$$\Omega_y = \frac{V_2 - V_1}{L} \quad (19)$$

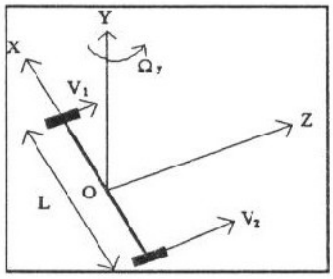

Figure n°5 : Kinematic of the axle which replace the machine

However, we just control δ (the wheel angle). There is a relation between R (the ray of the circle) and δ :

$$\tan\delta = \frac{b}{R} \quad \Rightarrow \quad \delta = \frac{b}{R} \quad (20)$$

because δ is very small (less than ten degrees)

With V the speed of the machine we have :

$$R = \frac{L \cdot V}{V_2 - V_1} = \frac{L \cdot V}{\Delta V} \quad (21)$$

Equations (19), (20) and (21) give us :

$$\delta = \frac{b \cdot \Omega_y}{V} \quad (22)$$

And then with (22) and (18) we have :

$$\delta = \frac{b}{V} \cdot \lambda \cdot \left(-\tan\alpha \cdot \left(\theta - \theta^*\right) + \left(\rho - \rho^*\right)\right) \quad (23)$$

λ is an empirical gain chosen equal to 0.1. In fact, we have the same gain applied to ($\theta - \theta^*$) and to the ($\rho - \rho^*$) terms. However, these physical magnitudes are very different (ρ is in meter and θ in radian). So we decided to adjust these magnitudes by different gains (K_1 , K_2) :

$$\delta = \frac{b}{V} \cdot \lambda \cdot \left(-K_1 \cdot \tan\alpha \cdot \left(\theta - \theta^*\right) + K_2 \cdot \left(\rho - \rho^*\right)\right)$$

which is the same equation than :

$$\boxed{\delta = \frac{b}{V} \cdot \left(-K_1 \cdot \tan\alpha \cdot \left(\theta - \theta^*\right) + K_2 \cdot \left(\rho - \rho^*\right)\right)} \quad (24)$$

With this equation we can control our machine with the visual data (θ and ρ) extracted directly from the image. They are the polar coordinates of the limit detected in the image.

III/ SIMULATION TESTS

In a first time we make simulation tests in which the machine has to reach a line one meter away (figure n°6).

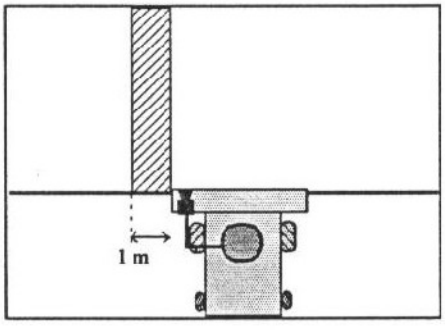

Figure n°6 : Simulation test conditions.

We have several test conditions which allow us to adjust our gains according to the wanted curve of response (figure n°7).
For our simulations, we choose a speed of 4 km/h and the range period is about 200 ms.

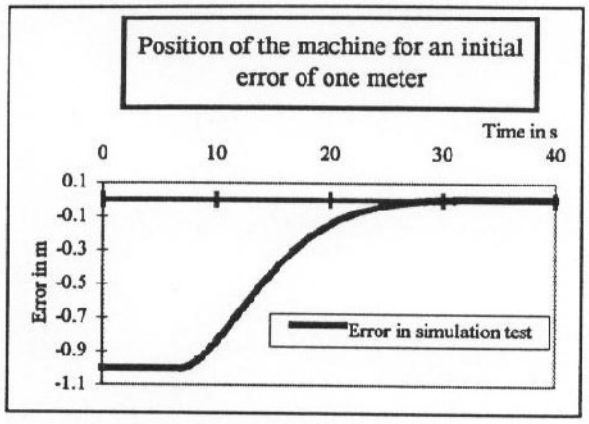

Figure n°7 : a simulation test at 4 km/h.

On this curve we have the machine error between its position and the line position. At 7 s we can see the response to the step. The gains are chosen with this curve and will not be changed. We take 7.9 for K_1 and 300 for K_2, which gives a response time about 20 s.

IV/ TESTS IN REAL CONDITIONS.

After the simulation tests it is interesting to make real tests. To do that, we decided to follow a white line on the ground to optimize the precision of the visual perception algorithm (figure n°8). In fact, with a white line, we have not any problem of perception because it is easier to detect than a limit between mowed and unmowed vegetation. We have thus made tests in various conditions (with or without noise) to different speeds and with a sampling period which changes by time.

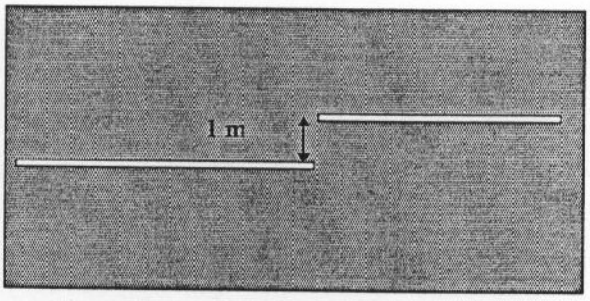

Figure n°8 : a view of the step on the ground.

The quality of our control servoing can be calculated in real time by using a second camera which is continuously measuring the distance between the vehicle and the white line.

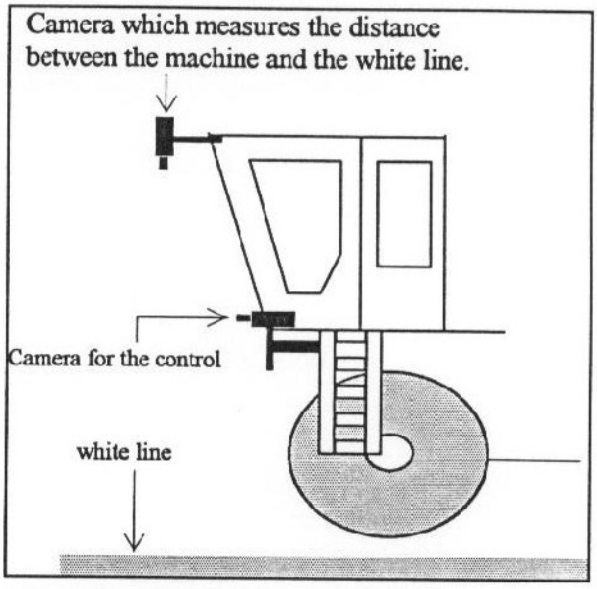

Figure n°9 : two camera, one for the system, the other to measure the result of the system.

The first curve is done with a speed of 4km/h and a range period of 200 ms which is the image processing calculation time (figure n°10). To make the simulation curve we introduce a delay which has the image processing calculation time value. So we can compare the simulation and the real curve which are done in the same experimental conditions.

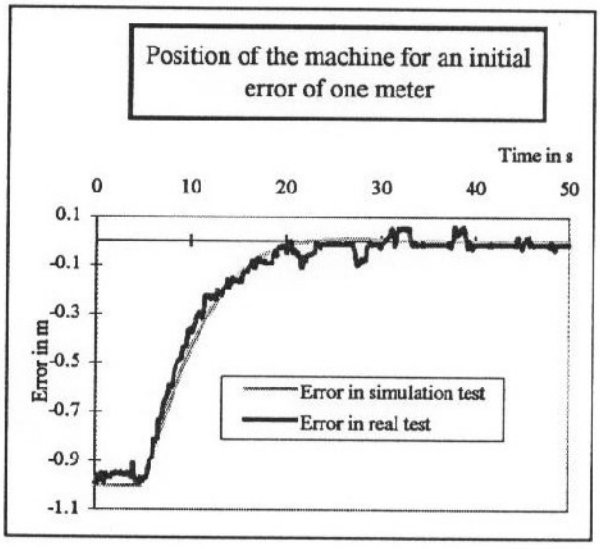

Figure n°10 : a real test at 4 km/h.

We can notice that the real and simulation curves are superimposed. The response time is about 20 s and there is not any overtaking. There is a lot of noise on the real curve because the camera which measures the distance between the vehicle and the white line vibrates a lot when the machine runs. The same image processing algorithm is used to control the machine and to measure the error. This algorithm has a precision of 5 cm. So the noise is produced by the camera and the image processing but not by the control system. We will see that noise have no consequence on our system.

The second curve is done with the same conditions but we introduce noise on the image processing. It is the same noise which is measured when the machine works in vegetation. The value of this noise is about 15 % (figure n°11).

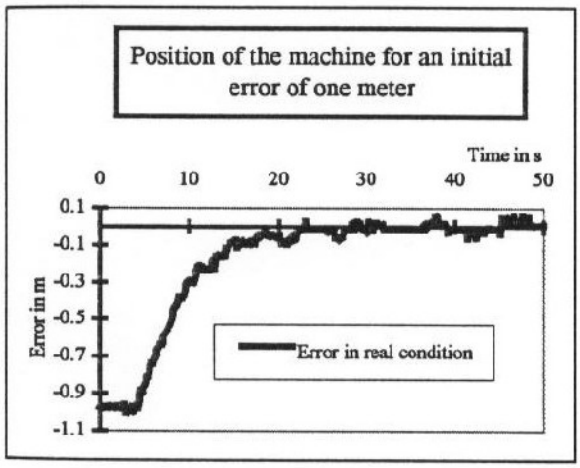

Figure n°11 : a real test at 4 km/h with 15 % of noise.

On this curve, it seems that there is no difference with or without noise. In fact the noise of the algorithm which is used to control the quatity of our system has more consequences than the effect of noise introduced in the result of the image processing. In simulation, with this noise, we can see a perturbation of 2 cm on the position of the machine.

The third curve is done with a speed of 8 km/h without noise (figure n°12).

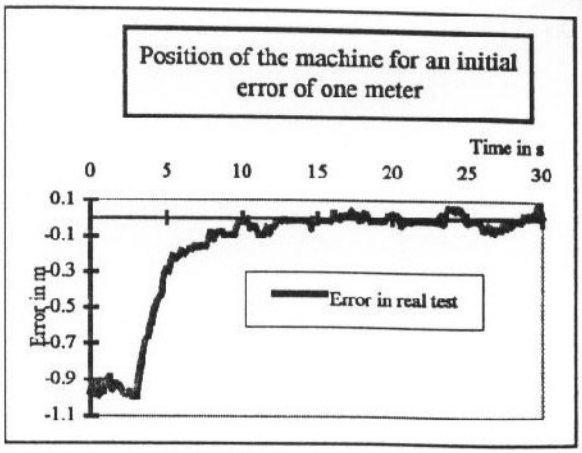

Figure n°12 : a real test at 8km/h.

Here the response of the machine (10 s) is faster than in the first case (20 s). In fact, the machine has the same trajectory but needs half the time to do it. The curve shows that the speed of 8 km/h doesn't change anything in the quality of our control.

CONCUSION.

In this article, we show that it is possible to control an agricultural mobile machine by a visual servoing approach. It is interesting to note that our machine is non-holonomic. We show that our theory can be used for a lot of machines whose trajectory at constant speed is a circle.
However, the regulation is done in movement and we do not solve the problem of control a non-holonomic machine with a final speed equal to zero.
Our gains are chosen thanks to a wanted curve of response and are not calculated like in the approach of Khadraoui [6]. In his approach, the gains are calculated according to the speed and the desired dynamic behaviour of the machine.

All our results show the robustness of our control algorithm. A noise of 15 % and a difference of speed of 100 % have no influence on the machine behaviour.
So in conclusion, we can say that our visual servoing approach, which avoids a 3D estimation, is a good way to control an agricultural mobile machine.

REFERENCES.

[1] M. Derras, "Segmentation non supervisée d'images texturées par champs de Markov : Application à l'automatisation de l'entretien des espaces natrurels". Thèse de doctorat de l'Université Blaise-Pascal, Clermont-Ferrand, Décembre 1993 (France).

[2] M. Derras, M. Berducat, P. Bonton, J. Gallice et S. Naudet, "Segmentation texturale originale Analyse et Parallelisation Temps réel", RFIA/AFCET, Reconnaissance des formes et intelligences artificielle, vol. 1, pp 133-144, janvier 1994, Paris.

[3] F. Chaumette, "La commande référencée vision : une approche aux problèmes d'asservissements visuels en robotique", Thèse de doctorat de l'Université de Rennes (France), juillet 1990, 171 pages.

[4] P. Rives et R. Pissard-Gibollet, "Asservissement visuel appliqué a un robot mobile : état de l'art et modélisation cinématique", Rapport de Recherche INRIA n°1577, Sophia Antipolis (France), décembre 1991, 42 pages.

[5] P. Tournassoud, "Planification et contrôle en robotique : application aux robots mobiles et manipulateurs", Hermes, Paris 1992, 248 pages.

[6] D. Khadraoui, C. Debain, P. Martinet, J. Gallice, and M. Berducat, "Vision Based Control Law for Agricultural Machines" : International Advanced Robotics Programme, the fourth Workshop on Robotics in Agriculture & the Food-Industry (October 30-31/1995), Toulouse (France).

[7] Klassen N.D., Wilson R.J., Wilson J.N. « Guidance systems for agricultural vehicles » : International Commission of Agricultural Engineering, XII World Congress on Agricultural Engineering, p 1136 to 1142, August 29 - September 1, 1994 Milano, Italy.

[8] D. Khadraoui, "Linear Control of High Speed Vehicle in Image Space", Second International Conference Industrial Automation, 7-9 june 1995, Nancy-France.

[9] C Samson, M le Borgne, B Espiau : Robot Control, The Task Function Approach. Oxford science publications, 1991, 364 p, ISBN 0-19-8538057